



OPEN

Application of multi-stage fracturing stimulation based on case study of Chang-7 shale gas formation in Ordos basin

Guang Dong¹, Yanping Lu²✉ & Shuai Dong¹

To address the issue of low production output, additional stimulation measures are always adopted. This study analyzes the complex characteristics of the Chang-7 shale gas reservoir in the central Tianhuan Syncline, Ordos Basin. Facing challenges from reservoir heterogeneity, we implemented a multi-stage fracturing pilot in the first horizontal well (DPX) of the Chang-7 reservoir using drillable bridge plug technology and customized fracturing designs based on horizontal well multi-stage stimulation theory and multi-fracture interference mechanisms. Research shows: Fracture parameters (stage count, geometry, length) and operational parameters (perforation scheme, fracturing scale, fluid type, injection rate) designed according to overall reservoir characteristics are significantly affected by heterogeneity during implementation, resulting in substantial variations in operational difficulty and outcomes across stages. Therefore, for reservoirs with strong heterogeneity, stage-specific designs must account for localized features to enhance success rates and production gains.

Keywords Chang-7 shale gas formation, Multi-stage fracturing, Fracture, Fracturing operations

Initial oil&gas production rates from tight sandstones and shales are typically low. Additional stimulation measures are required to enhance production efficiency¹. Fracturing technology is widely used to improve the recovery rate of oil and gas reservoirs^{2,3}. Current commonly used fracturing technologies in shale reservoirs include horizontal well multi-stage fracturing and simultaneous multi-well fracturing, among others⁴. Horizontal well multi-stage fracturing serves as the core technology for stimulating low-permeability reservoirs. Its value lies in significantly enlarging the drainage area and Stimulated Reservoir Volume (SRV) by creating multiple fracture clusters along the horizontal lateral^{5,6}. This process reconstructs flow pathways and substantially enhances well productivity. Numerical simulation methods are extensively employed in the engineering design of horizontal well multi-stage fracturing. Through simulation calculations, they provide critical references for determining fracturing treatment parameters. During the execution of horizontal well multi-stage fracturing, inter-fracture interference occurs in aspects such as fracture propagation, stress field distribution, and flow field distribution. It has been witnessed that the combination technique of horizontal well and multi-stage fracturing stimulation does well in case of exploitation of tight formation in Ordos basin of China. However, the development of shale gas in Ordos basin is still in the primary exploration stage. Extensive research exists on horizontal well fracturing for tight sandstone gas reservoirs in the Ordos Basin, and studies on the mechanisms of multi-stage fracturing in horizontal wells are relatively comprehensive. However, case studies on the development of Chang 7 shale gas remain limited, with a particular scarcity of field fracturing trials. Current understanding of the optimal design and production mechanisms for this reservoir is insufficient, necessitating urgent engineering case studies. This paper presents a multi-stage fracturing pilot test conducted on the DPX well—the first horizontal well targeting the Chang 7 shale gas interval in the central Tianhuan Syncline of the Ordos Basin. Based on analysis of Chang 7 reservoir characteristics, fracturing parameters were simulated. Integrating previous operational experience with analogous techniques, the fracturing treatment design was optimized. The effectiveness of the stimulation treatment in the Chang 7 shale gas reservoir was evaluated. The results provide critical reference for optimizing fracturing design parameters in shale gas reservoirs across the Ordos Basin. As China's second-largest sedimentary basin, the Ordos Basin possesses significant hydrocarbon exploration potential. The Triassic Yanchang Formation Chang 7 contains widely developed organic-rich source

¹Henan Mechanical and Electrical Vocational College, Zhengzhou 451192, Henan, China. ²School of Artificial Intelligence, Beijing Institute of Economics and Management, Beijing 100102, China. ✉email: yanpinglu@biem.edu.cn

rocks, covering an area of $(4\text{--}5)\times 10^4$ km². This source rock unit exhibits high Total Organic Carbon (TOC), predominantly Type I-II₁ kerogen, with vitrinite reflectance (Ro) values primarily ranging from 0.9 to 1.2%, indicating a thermally mature stage. Its substantial volume of retained hydrocarbons provides the essential material basis for large-scale shale hydrocarbon accumulation⁷. The Chang 7₃ sub-member shale is characterized by clay-rich mineral composition. The Chang 7₂ sub-member has higher clay mineral content than Chang 7₁. The dominant pore types in these three sub-members are dissolution pores, intergranular pores-dissolution pores, and intergranular pores, respectively. Accordingly, the reservoir quality is classified as Type I (Excellent), Type II (Medium), and Type III (Poor). Six distinct source-reservoir configurations are identified: (1) Superb source rock-Poor reservoir, (2) Medium source rock-Excellent reservoir, (3) Poor source rock-Medium reservoir, (4) Medium source rock-Medium reservoir, (5) Superb source rock-Medium reservoir, and (6) Poor source rock-Excellent reservoir. Hydrocarbon enrichment is highest in the Chang 7₃ sub-member, followed by Chang 7₂, while Chang 7₁ is unfavorable for shale hydrocarbon accumulation. Shales with high TOC and high thermal maturity exhibit excellent hydrocarbon generation potential. High clay content and favorable pore connectivity facilitate hydrocarbon migration and accumulation. The source-reservoir configuration ultimately controls the location of shale hydrocarbon enrichment⁸.

Well (DPX) is geologically located in the Quanwanzi uplift position in the middle section of the Tianhuan Syncline in the Ordos Basin. The reservoir belongs to the Yanchang Formation in the Mahuangshan West block, which is a deep lake-semi-deep lake sedimentary environment in the lake basin. The northeastern part is located in the most developed area of mud shale in the lake basin, with the thickness of effective source rocks reaching more than 90 m, good quality, and high hydrocarbon generation potential. We focus on the methods of effective mining and performance evaluation, based on the Multi-stage Fracturing experiments in field of first horizontal well named DPX drilled in Chang-7 shale gas formation in the middle part of the Tianhuan syncline in Ordos basin. Novel fracturing fluid and optimal design is proposed and put into practice. The research announces that the fracturing difficulty of Chang-7 shale gas reservoirs is significantly higher than that of Chang-8. The reservoir characteristic along the horizontal well is different. The results of the total eight stages are different from each other and there is no regularity to follow. We really gather experiment confronting with technical problems such as high injection pressure and frequent sand plug. The practice announced that some methods, so as steeply plugging the proppant, increasing proppant concentration tentatively, will reduce the risk and improve the success rate of hydraulic fracturing. The treatment experience of well DPX may offer reference for further exploitation of shale gas reservoir in Chang-7.

Reservoir formation characteristics

In DPX well, the main oil&gas reservoirs are Yanchang Series including Chang-7 and Chang-8 and Yanan Series. However, Yanan Series and Chang-8 are sandstone reservoirs. And parts of Chang-7 have the shale gas reservoirs. In field we firstly drilled a parameter well before drilling the DPX. Data acquired from Parameter Well confirmed that Chang-7 gas reservoir is worth mining. The Chang-7 shale exhibits great thickness, high TOC, and favorable hydrocarbon generation potential⁷. Source rocks primarily develop in the lower section, with total hydrocarbon shows exceeding 20% in mid-lower intervals. Gas-bearing cores total 34.11 m, confirming the Chang-7 shale as the target for fracturing. Therefore, we drilled a horizontal well and taking Multi-stage Fracturing which is helpful for exploring reservoir characteristics and potentiality.

The logging of DPX pilot well reveal that the thickness of Chang-7 reservoir is about 101 m. The formation is dominated by gray-black carbonaceous shale and the upper part of the formation is gray-black mudstone. The formation is a gas reservoir. Six intervals of formation rock were cored at the vertical direction of Chang-7 reservoir. The footage was 42.59 m and the core recovery was 99.32%. The length of oil bearing core was 1.18 m and the gas bearing core was 34.11 m. The well logging shows that the Chang-8 reservoir which is vertically 10 m below the Chang-7 reservoir is oil-water layer. The pore pressure coefficient in Chang-7 reservoir is between 0.832 and 0.983 and the range of formation temperature is 80–90°C.

FMI (Fig. 1) indicates laminations in high-sand content formations and induced/natural fractures, while high-clay formations lack lamination. Cross-cutting horizontal micro-fractures are developed.

SEM (Fig. 2) reveals: (a) Vertical to bedding: Clay minerals show preferred orientation with developed micro-fractures between flakes; (b) Parallel to bedding: Smooth bedding planes with cleavage features, indicating well-developed shale laminations prone to failure along bedding. Mineral shrinkage fractures are observed in both views, while structural/bedding fractures are underdeveloped. Based on SEM analysis, the shale microfractures in this interval are predominantly characterized by interclay platelet microfractures and mineral shrinkage fractures.

Imaging log (FMI) and core SEM scanning results indicate that natural fractures in the Chang 7 reservoir of Well DP-1 are well-developed, facilitating the formation of a Fracture Network System (FNS).

According to the analysis of the physical properties of the cores, the porosity of the formation rock is less than 1%, and the average permeability is approximate to 0.03 mD. Core X-ray diffraction analysis: Quartz (avg. 31%) and clay minerals (avg. 63%) dominate with stable distribution; carbonate content is low (avg. 0.56%) and highly variable; clays are mainly illite (avg. 61%) with 10% illite/smectite mixed-layer and no smectite. The content of clay minerals is 62.56%. In general, the brittleness of the Chang-7 reservoir is low, so it difficult for the generation of network fracturing in the reservoir.

Sondergeld et al. proposed a method for calculating brittle mineral content using Eq. (1)

$$\beta = \frac{C_{quartz}}{C_{quartz} + C_{clay} + C_{carbonate}} \quad (1)$$

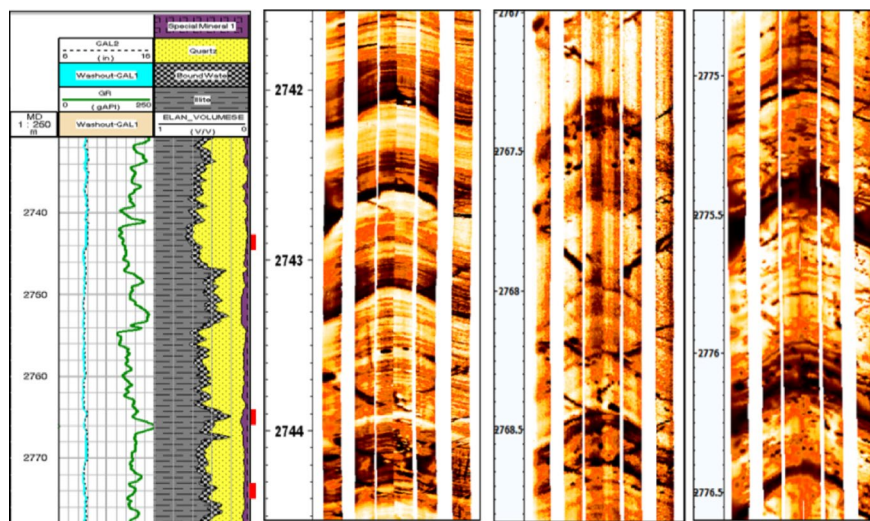


Fig. 1. The FMI bedding characteristic of the pilot well.

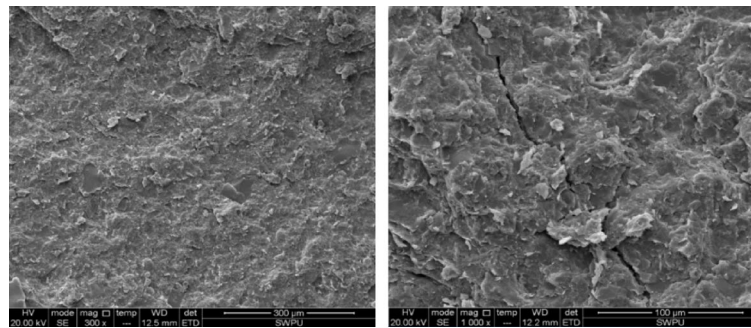


Fig. 2. The SEM of Chang-7 sample. (a) the original Chang-7 sample shows smooth bedding planes; (b) sample preparation for Chang-7 with artificial cracks.

	TOC
Position	2744.8–2764.8 m
Range (%)	1.85 ~ 3.09
Average (%)	2.31
	2765.8–2773.8 m
	2.35 ~ 3.68
	3.26

Table 1. TOC test results.

β —Brittle mineral content, %; C_{quartz} —Quartz mass fraction in shale, %; C_{clay} —Clay mineral mass fraction in shale, %; $C_{\text{carbonate}}$ —Carbonate mineral mass fraction in shale, %.

Calculations using Eq. 1 show:

Brittle mineral content of quartz-only lithofacies: 26–39%. Brittle mineral content of quartz-carbonate lithofacies: 31–41%. The overall low brittle mineral content indicates poor rock brittleness in the Chang-7 reservoir. Consequently, it is difficult to develop an effective fracture network system during stimulation treatments.

The Total Organic Carbon (TOC) value of the target formation is varying between 1.85% and 3.68%, which is one of the important indicators for evaluating the quality of shale gas reservoirs. It is usually considered that the reservoir is high quality when the TOC is between 1.9 and 5.15%. In the case, the observed value is shown in Table 1. Here the average value of TOC is higher than 2%, which means the organic matter in shale is relatively abundant. Vitrinite reflectance (R_o) ranges from 0.82 to 1.01%. We usually expected the vitrinite reflectance is higher than 0.5%.

According to the mechanical testing, we draw the conclusion that the rock of Chang-7 reservoir is characterized as low elastic modulus of 17,600 MPa and low Poisson's ratio of 0.21. And the variation coefficient of in-situ stress is 0.307.

The optimization of parameters

Technical difficulties

The complex geological characteristics and high heterogeneity of reservoirs pose significant challenges to hydraulic fracturing operations⁹. The difficulties in fracturing mainly lies in the following aspects.

(1) The formation is not rich in oil & gas while the physical properties are undesirable. Big scale of hydraulic fracturing is needed to increase SRV as much as possible¹⁰⁻¹³.

(2) There are the carbonate salt filling strip in High angle fractures, while the big difference between the in-situ stress is an adverse factor for the generation of network fracture when fracturing^{14,15}.

(3) The presence of stress sensitivity and high content of clay minerals will cause more serious of imbedding of proppant, which dramatically influence the conductivity of the induced fractures^{16,17}.

(4) The existence of high angle natural fracture will increase the fracturing fluid filtration because the formation pressure is low. It will increase the difficulty of viscosity break of crosslinked and the fluid flowback^{18,19}.

Parameter setting of stage number

Multi-stage fracturing reconstructs flow fields to overcome injectability and productivity challenges in low-permeability reservoirs. Its mechanism involves: Physical fracture creation (increasing contact) → Mechanical stabilization (proppant resistance) → Seepage enhancement (reducing resistance). Fracture design relies on in-situ stress control, fracture mechanics, and fluid-solid coupling. Fracture orientation follows minimum horizontal stress; spacing is constrained by stress shadowing; length is limited by rock toughness. Fracture propagation exhibits viscous- and toughness-dominated regimes. Multi-fracture competition involves stress interference, fluid competition, and rock damage. Proppant embedding reduces conductivity. Design must balance in-situ stress, fracture energy thresholds, and dynamic coupling.

Here factors affecting the productivity of multi-section fractures in staged fracturing of horizontal wells. different stage number of fracturing is simulated and we assumed each stage leads two bunches of fractures.

When the multi-stage fracturing exceeds 7-stage, the increase of the cumulative production becomes slower(Figs. 3 and 4.). Drawing on Sinopec North China Oil & Gas Company's field experience in this region, multi-stage fracturing in horizontal wells penetrating tight sandstone reservoirs of the Ordos Basin typically utilizes 6-12 stages. Given that increased stage count elevates technical complexity and costs, this stimulation pilot prioritized cost-effectiveness, risk reduction, and operational feasibility. Integrated with software-derived production simulation under variable stage configurations and comprehensive field constraints analysis, an 8-stage fracturing design was selected as the optimal solution (Figs. 3 and 4).

Parameter optimization of the fracture's distribution

Setting the number of stage as 8, then we can carefully contrast the the productivity with different fracture's distribution. There follows the analysis of distributions of uniform type, W-type, U-type, and long fracture of ends type (ends type).

Numerical simulation modeled production performance under varying fracture distribution patterns. As illustrated in Figs. 5, 6 and 7, the results demonstrate that the W-shaped configuration delivers the highest daily and cumulative production rates, whereas the uniform pattern yields the poorest performance. Therefore, W-type is the recommended distribution, and the result is shown in Fig. 8. The amount of proppant for stage 2, stage 4, stage 6 and stage 8 should be increased to generate a larger scale fracture²⁰.

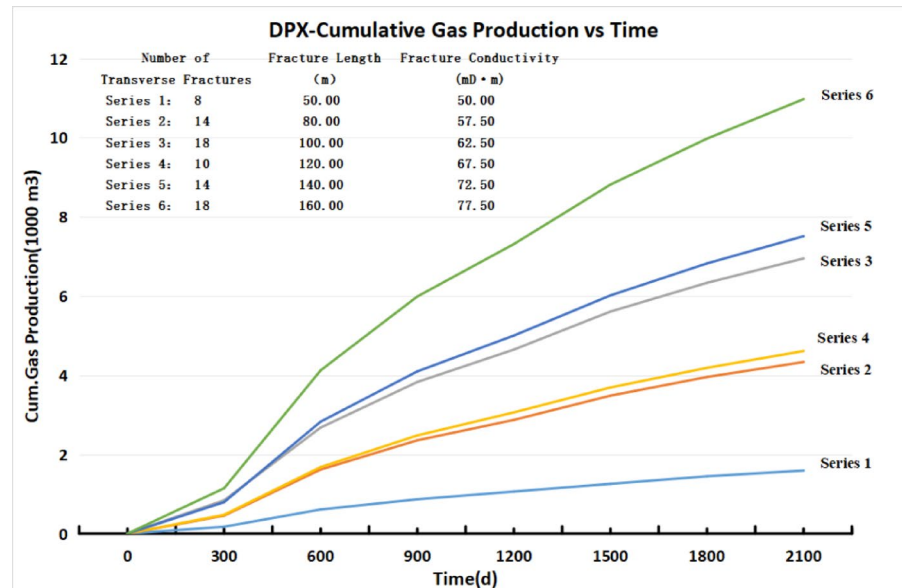


Fig. 3. The daily production VS time with different number of fracturing stage.

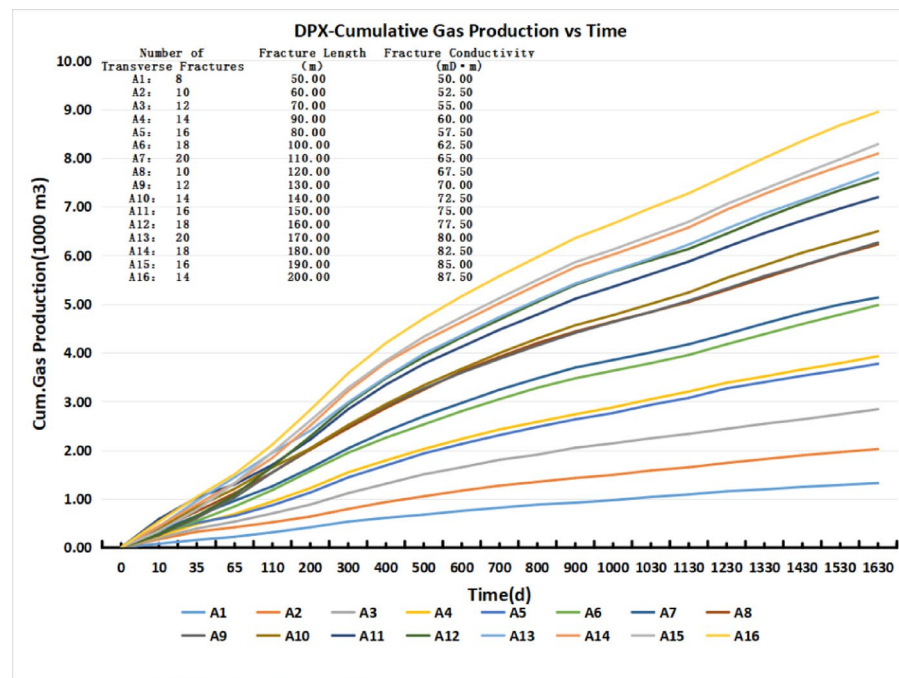


Fig. 4. The cumulative production VS time with different number of fracturing stage.

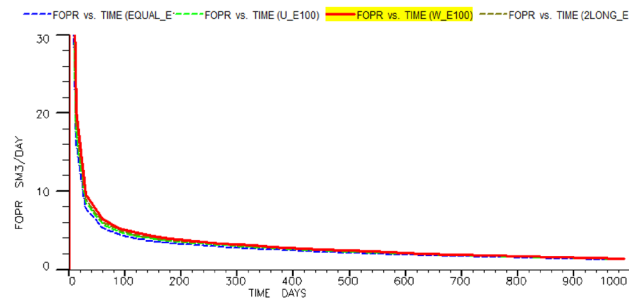


Fig. 5. The daily production of different fracture distribution.

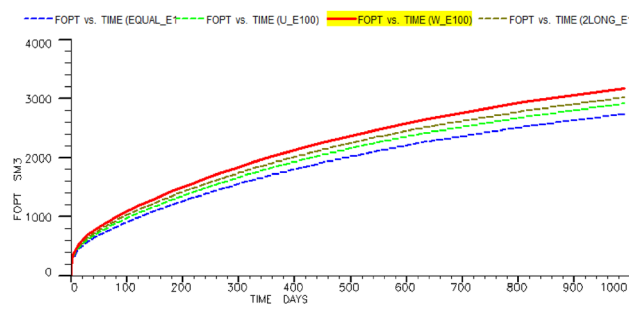


Fig. 6. The cumulative production of different fracture distribution.

Parameter optimization of half-length of the fracture

With the condition of 8-stage fracturing, we conducted the numerical simulation experiments to optimize the half-length of the fracture. Here the half-length is range from 80 m to 280 m with step factor of 40 m.

The simulation result shows in Figs. 9, 10 and 11. The results indicate that longer fracture half-lengths correlate with higher production, but the incremental production gain diminishes with increasing half-length. When the fracture half-length exceeds 200 m, the growth rate of the cumulative production significantly declines.

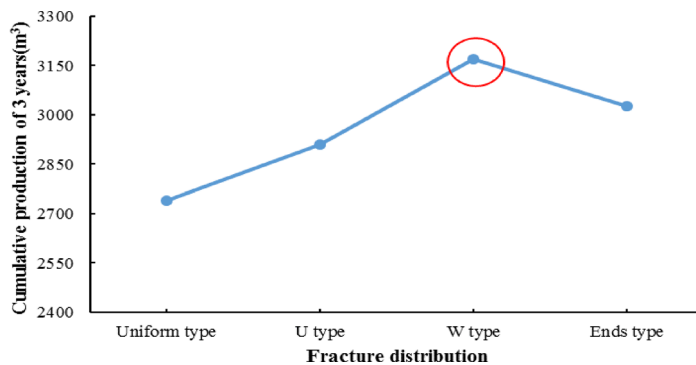


Fig. 7. Cumulative production of 3 years with different fracture distribution.

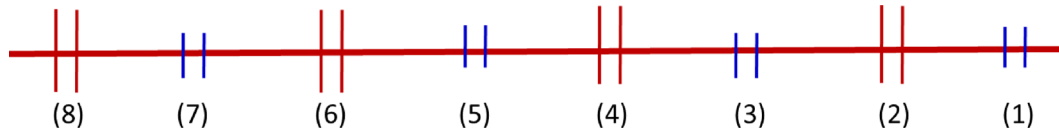


Fig. 8. Fracture distribution of W-type.

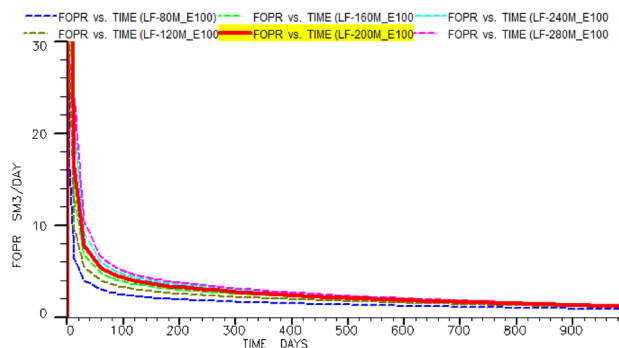


Fig. 9. The daily production VS time with different value of half-length.

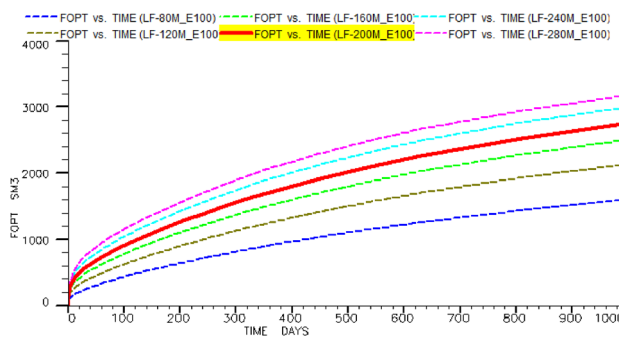


Fig. 10. The cumulative production VS time with different value of half-length.

Considering operational constraints, the optimal fracture half-length is recommended to range between 160 m and 200 m.

Parameter optimization of operation parameters

(1) Fracturing Scale Optimization.

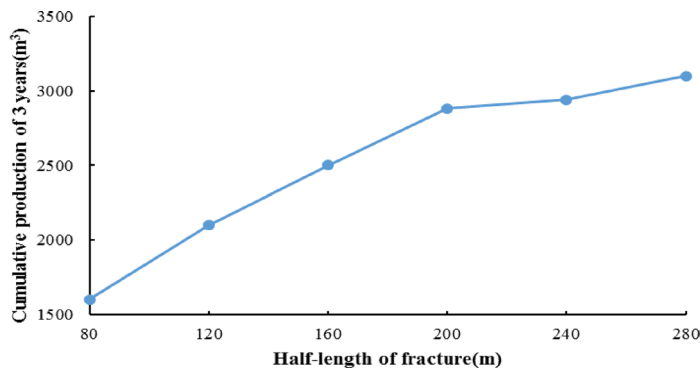


Fig. 11. The cumulative production of 3 years with different half-length fracture.

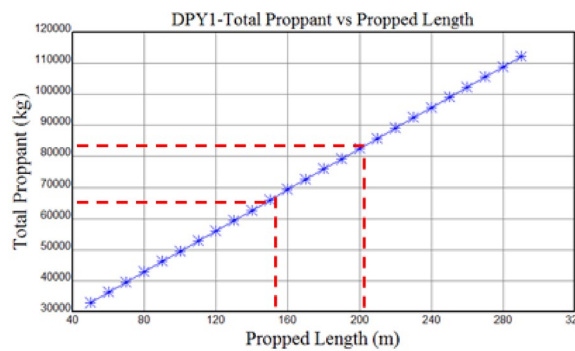


Fig. 12. The propped length VS total proppant with the optimal flow conductivity.

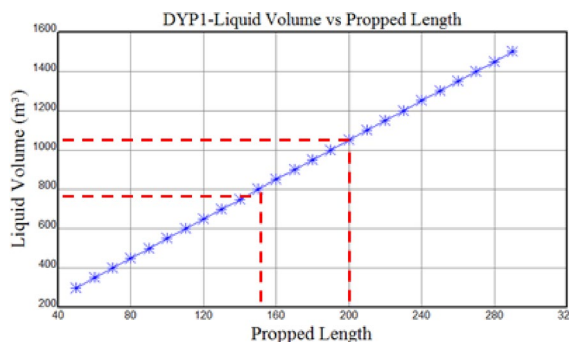


Fig. 13. The propped length VS liquid volume with the optimal flow conductivity.

Considering the feasibility of field application, here we assume half-length ranges between 160 m and 200 m, the volume of proppant is about 40–50 m³ for one segment, and the quantity of fracturing fluid is about 800 m³ for one treatment. The simulation illustrated in Figs. 12 and 13.

(2) Flow Rate Optimization.

In the high sand ratio conditions, fracturing process, crosslinked gel fracturing fluid solution is always accepted. Software simulations constrained by the maximum safe pressure ratings of fracturing pumps, surface lines, and valves project wellhead pressures between 42 MPa and 52 MPa when implementing pumping rates of 8–12 m³/min shown in Fig. 14. The most appropriate flow rate is between 8 m³/min – 12 m³/min shown in Fig. 15. And Fig. 16 is the geometry of the fracture predicted.

The magnitude of wellbore pressure and net pressure inside the fracture is closely related to the fracturing construction displacement. As shown in Figures, there is non extended clustering at low displacement, while high displacement corresponds to high net pressure within the fracture, increasing the possibility of multiple

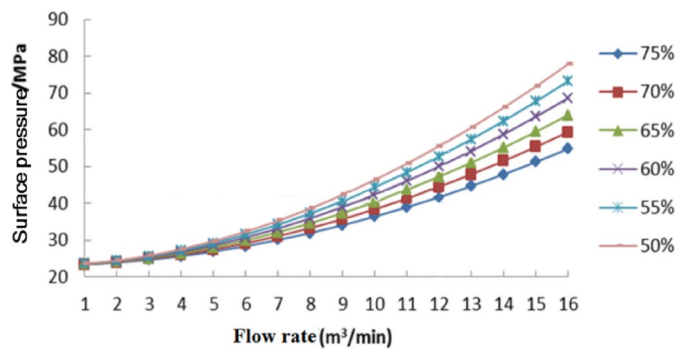


Fig. 14. The prediction of wellhead pressure with different reduction efficiency of friction resistance.

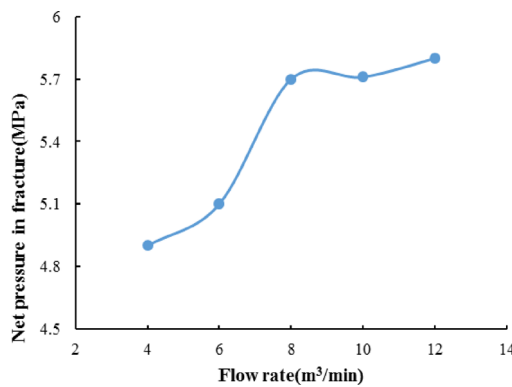


Fig. 15. The Maximum net pressure in a fracturing stage with different flow rate.

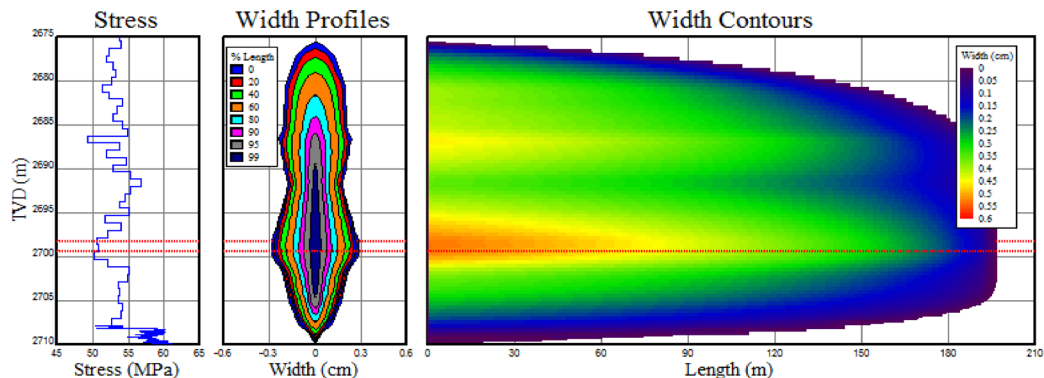


Fig. 16. The geometry of the fracture.

cluster cracks initiating and effectively expanding. Increasing displacement is beneficial for promoting the expansion of each cluster crack.

Cases of fracturing operation

Fracture treatment design

In the field of petroleum engineering, multistage fracturing in horizontal wells is a core technology for the economical and efficient development of unconventional oil and gas resources (such as shale gas, shale oil, tight gas, tight oil, etc.). Current mainstream horizontal well fracturing techniques and their geological applicability are categorized as follows:

(1) Plug-and-Perf Fracturing.

Principle: A bridge plug is run via wireline or coiled tubing to isolate previously fractured stages. The new stage is perforated with a gun and fractured. This process is repeated. Bridge plugs are categorized as drillable (removed by drilling later) or dissolvable (self-degrading).

Applicability: Long horizontal sections: Flexible stage count. Highly heterogeneous reservoirs: Allows arbitrary adjustment of perforation locations for targeted stimulation of sweet spots. Applicable to shale oil/gas development; serves as the backbone technique of the North American shale revolution.

Advantages: Precise staging, strong adaptability; dissolvable plugs eliminate milling, protecting the reservoir.

Limitations: Long operational cycle; wireline perforation requires multiple pump-down operations; plug drilling adds cost (except for dissolvable plugs).

(2) Sleeve Staged Fracturing.

Principle: Multiple fracturing valves with sleeves are pre-installed on the casing. Sleeves are sequentially opened by dropping balls (of different diameters) or via coiled tubing (CT), enabling stage-by-stage fracturing.

Applicability: Shale Gas/Shale Oil: Preferred for large-scale factory-mode operations; suitable for long horizontal sections. Tight Sandstone: Enables rapid and efficient staging; ideal for blocks with good reservoir homogeneity where precise location control is unnecessary.

Advantages: High operational speed, low cost; enables one-time completion of multistage fracturing.

Limitations: Gradual reduction in sleeve inner diameter restricts future production tubing; inability to precisely control fracture location.

(3) Coiled Tubing Hydratjet Perforating & Fracturing.

Principle: Utilizes a jetting tool conveyed by coiled tubing. High-velocity water jets perforate the formation and leverage the “jet-induced pressure boosting effect” (dynamic isolation) to initiate fracturing directly. Multistage operations are completed by pulling the tool up stage by stage.

Applicability: Open-hole or Cased Hole: Particularly suitable for uncased horizontal wells. Thin Interbeds/Complex Lithology: Allows precise targeting of fracture points, avoiding faults or water zones. Low-Pressure Reservoirs: Eliminates need for mechanical isolation, avoiding packer setting difficulties.

Advantages: No need for plugs or sleeves, enabling full-bore production; flexible operations.

Limitations: Longer operational cycles, higher cost; higher risk of screenout.

(4) Mechanical Packer Isolation Fracturing.

Principle: Multiple mechanical packers (e.g., inflatable or compression-set) are assembled in series on the fracturing string. Stages are isolated by the packers, allowing sequential fracturing.

Applicability: Medium-to-Short Horizontal Sections: Economically efficient when stage count is low. Carbonate Reservoirs: Commonly used in acid fracturing operations; packers exhibit strong acid resistance.

Advantages: Single-trip string run enables continuous operations; no ball seat restrictions, providing large bore access.

Limitations: High risk of stuck pipe; low efficiency for long horizontal sections; requires high wellbore quality.

(5) Diverted Fracturing with Temporary Plugging Agents.

Principle: Temporary plugging agents (e.g., balls, particulates) are pumped during a single fracturing treatment to seal existing fractures. This diverts fluid to new zones, achieving “infinite-stage” fracturing.

Applicability: Naturally Fractured Zones: Leverages natural fractures to create complex fracture networks. Re-fracturing of Old Wells: Activates unstimulated zones.

Advantages: No need for staging tools, reducing cost; suitable for complex fracture network stimulation.

Limitations: Diversion effectiveness is difficult to predict; plugging agents may cause reservoir damage.

Horizontal well multi-stage fracturing technology has been extensively deployed in tight sandstone reservoirs across the Ordos Basin^{21–23}. These field applications provide substantial operational benchmarks for designing fracturing parameters in Well DPX. Integrating historical fracturing experience from horizontal wells in the Ordos Basin while comprehensively evaluating Well DPX’s reservoir geological characteristics, development costs, and engineering risks, drillable plug-and-perf staged fracturing was selected for the multi-stage stimulation pilot. Subsequent fracturing treatment parameters were designed accordingly^{24–26}. 8-stage fracturing is applied with two clusters in stage of the second, third, fourth, fifth and the eighth stages, shown in Fig. 17 and the detail parameters illustrated in Table 2. Here long cluster type is used with a perforation length of 1.5–3 m per cluster, larger aperture perforations are adopted to reduce perforation friction.

It is important to implement acid pretreatment according to the well completion and the mini fracturing test situation. In the initial stag, variable flow rate, variable viscosity, and pre ceramic proppant technology is taken

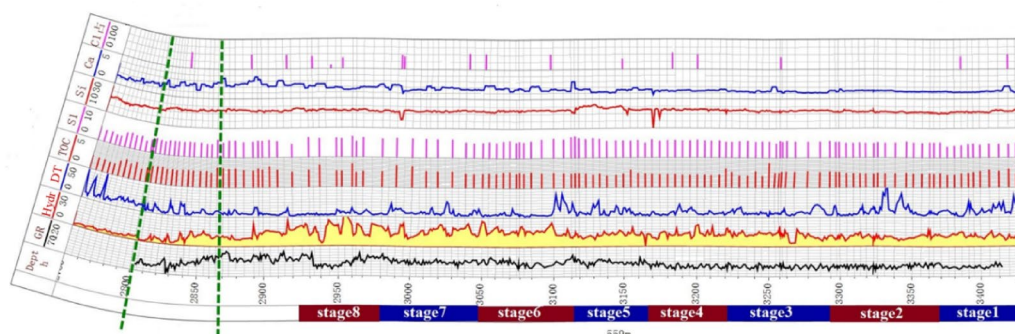


Fig. 17. Fracture placement along the DPX well.

Bunch of perforation	2
The length of each bunch(m)	3
The distance between two bunches(m)	15~30
Perforation phase(°)	60
Perforation density(hole/m)	20
Perforation diameter(mm)	9.5
Perforation per bunch	60
Total perforation holes	120

Table 2. Well DPX perforating parameter.

Item	pH	Density g/cm ³	Surface tension mN/m	Anti-swelling rate %	The damage rate %	170s ⁻¹ viscosity mPa.s
SRFR-1	7.05	1.005	24.6	85	10	1.5~3.0

Table 3. The main properties of slickwater.

Concentration of thickening agent	Viscosity of the base fluid mPa.s	Viscosity of the crosslinked fluid mPa.s	Reduction efficiency of friction resistance
0.1%SRFP-1	8.5	19.5	60%
0.2% SRFP-1	15.6	25.1	62%
0.3% SRFP-1	30.8	52.3	63%
0.35% SRFP-1	33.0	60.1	-
0.40% SRFP-1	42.1	68.7	-

Table 4. The properties of crosslinked fluid with different concentration of thickening agent.

to control the fracture height and ensure the propagation of main fracture, usually the flow rate is controlled between 8 m³/min and 12 m³/min²⁷.

The new fracturing fluid adopts a combination of crosslinked fluid and slickwater. Compared with the traditional fracturing fluid containing only crosslinked fluid, it is more suitable for fracturing stimulation of the Chang-7 shale gas reservoir. The action process of the fracturing fluid is as follows: crosslinked fluid is pad fluid, slickwater is used to generate micro fracture, and the crosslinked fluid is used to carry sand at the last period of the process. The Fracturing treatment is implemented with liquid nitrogen to Improve the flowback effect. The injection of proppant is not continuous but intermittent. The optimum range of fracture fluid volume of each stage is between 800 m³ to 1000 m³. Due to high clay content, the fracturing fluid system should be adjusted to inhibit the expansion of clay. Tables 3 and 4 represent the property of crosslinked fluid and slippery water.

Considering the closure stress, proppant pressure resistance, crushing rate, conductivity and other factors, the proppant combination is as follows: 100 mesh ceramsite, 30/50 mesh ceramsite and 20/40 mesh ceramsite^{20,28}.

Fracturing operation

In the total eight stages of fracturing, three of them are easily approached, whereas more difficult conditions with high pressure and sand plug are confronted in the other five.

(1) Instance 1.

Stage 1 (Fig. 18): Injection process and slug sand-group pack technique are adopted. Slickwater and crosslinked fluid are used alternately. In particular, 440 m³ slickwater are injected, following with 374 m³ crosslinked fluid and 16 m³ acid, totally 40.1 m³ proppant are used.

Stage 2 (Fig. 19): Injection process: plug type. Fluid injection type: slickwater and crosslinked fluid are used alternately with 430 m³ slickwater, 430 m³ crosslinked fluid and 10 m³ acid, 53 m³ proppant.

Stage 6 (Fig. 20): Due to the high treatment pressure, the injection process is different from stage1 and stage2. Injection process: multistep type with variable proppant concentration(The ratio of proppant and carrier fluid). Fluid injection type: slickwater and crosslinked fluid are used alternately with 493 m³ slickwater, 700 m³ crosslinked fluid and 13 m³ acid, 42 m³ proppant.

(2) Instance 2.

Lots of difficult conditions with high pressure and sand plug are confronted in the stage 3, stage 4, stage 7 and stage 8. In the stage 3, when the 3% proppant concentration is injected into formation, the treatment pressure rise rapidly until exceed the limiting safe pressure (Figs. 21 and 22) 0.23 m³ proppant is injected after blowing off, reperforating and well clean-up(with coiled tubing).

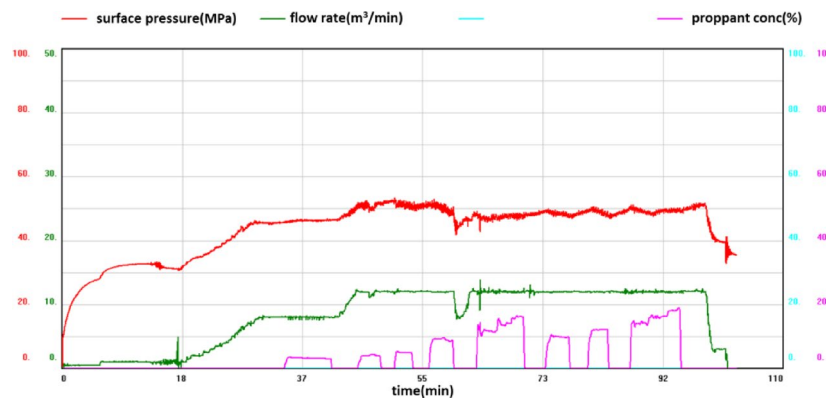


Fig. 18. Treatment data of stage 1.

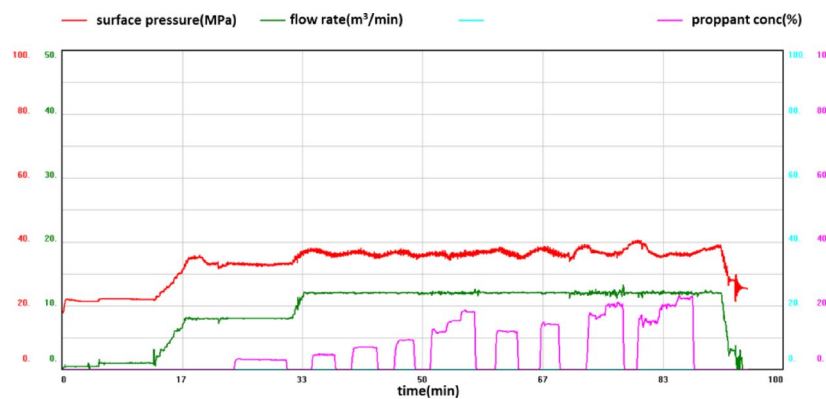


Fig. 19. Treatment data of stage 2.

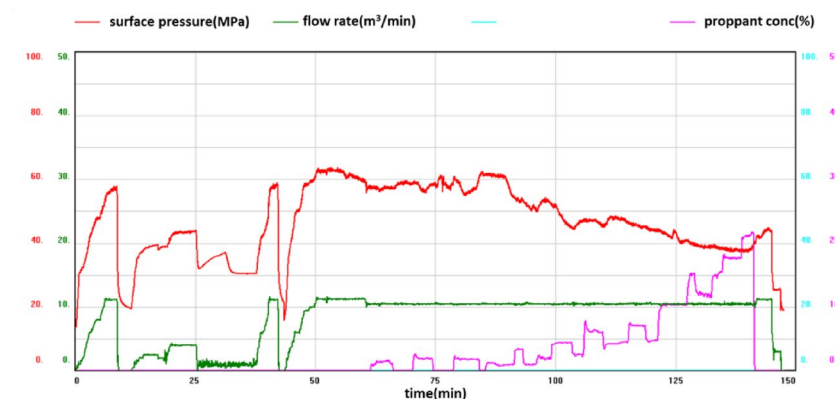


Fig. 20. Treatment data of stage 6.

Conclusions

Based on the multi-stage fracturing experiment of Well DPX and combined with the main characteristics of the Chang-7 reservoir, the study concludes that:

- (1) The heterogeneity of reservoir characteristics leads to differences in the construction difficulty of each stage of multi-stage fracturing. When designing a fracturing scheme, the reservoir characteristics at the location of fractures in each stage should be fully recognized, and personalized fracturing construction schemes should be designed for each stage to improve the fracturing success rate.
- (2) According to the analysis of on-site construction results from this fracturing experiment, the stronger the plasticity of the target fracturing interval, the greater the fracturing fluid filtration loss, and the more difficult it is to create fractures, which results in insufficient fracture creation (too narrow fracture width).

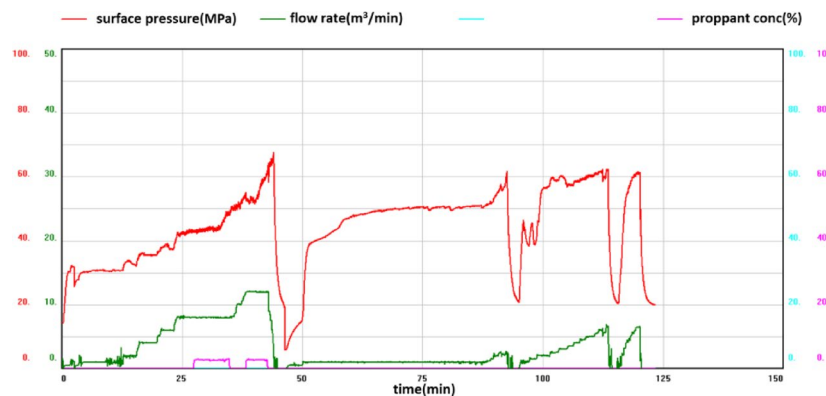


Fig. 21. Treatment data of stage 3(the first time).

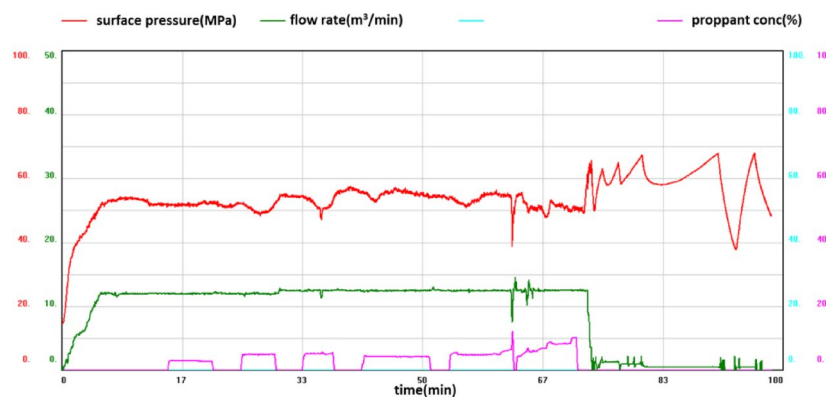


Fig. 22. Treatment data of stage 3(the second time).

(3) When implementing multi-stage fracturing for shale gas reservoirs, target reservoirs with higher brittleness indices should be preferentially selected to enhance the stimulation effect.

DPX is the first horizontal well drilled in Chang-7 shale gas formation in the middle part of the Tianhuan syncline in Ordos basin. The experience of Multi-stage Fracturing for this well can provide a reference for the further development of Chang-7 shale gas formation.

Data availability

All data generated or analysed during this study are included in the supplementary information files.

Received: 25 March 2025; Accepted: 21 July 2025

Published online: 26 July 2025

References

1. Liu, H. et al. October. Advanced Completion and Fracturing Techniques in Tight Oil Reservoirs in Ordos Basin: A Workflow to Maximize Well Potential. Paper SPE presented at the SPE Annual Technical Conference and Exhibition, San Antonio, Texas, USA, 8–10 (2012).
2. Li, X., Wang, H., Zhang, Y. & Liu, C. The crack propagation behaviour of CO₂ fracturing fluid in unconventional low permeability reservoirs: Factor analysis and mechanism revelation. *J. Petrol. Sci. Eng.* **218**(Part B), 111032 (2023).
3. Chen, J. et al. Wellhead stability during development process of hydrate reservoir in the Northern South China sea: evolution and mechanism. *China Ocean. Eng.* **38** (1), 1–15 (2024).
4. Belyadi, H., Fathi, E. & Belyad, F. *Hydraulic Fracturing in Unconventional Reservoirs: Theories, Operations, and Economic Analysis* (Elsevier, 2019).
5. Liao, S., Hu, J. & Zhang, Y. Investigation on the influence of multiple fracture interference on hydraulic fracture propagation in tight reservoirs. *J. Petrol. Sci. Eng.* **211**, 110160 (2022).
6. Yan, Z. et al. A coupled matrix-fracture productivity calculation model considering low-velocity non-Darcy flow in shale reservoirs. *Fuel* **357**, 129845 (2024).
7. Wu Kai, G. et al. *Petroleum Geol. Exp.* **46**(06), 1298–1311 (2024).
8. Wu Jia, Z. & Weiwei, L. *Yuchen Et Al Lithologic Reservoirs*, **37**(01): 170–181. (2025).
9. Saldungaray, P. M. & Palisch, T. T. Hydraulic Fracture Optimization in Unconventional Reservoirs. Paper SPE presented at the SPE Middle East Unconventional Gas Conference and Exhibition, Abu Dhabi, 23–25 January 2012.
10. Wang, H. et al. June. The Study of CO₂ Flooding of Horizontal Well with SRV in Tight Oil Reservoir. Paper SPE presented at the SPE Biennial Energy Resources Conference, Spain, Trinidad, 09–11 (2014).

11. Zhao, G. A Simplified Engineering Model Integrated Stimulated Reservoir Volume (SRV) and Tight Formation Characterization With Multistage Fractured Horizontal Wells. the SPE Canadian Unconventional Resources Conference, Calgary, 30 October-1 November (2012).
12. Zeng, J. et al. Analytical solutions for multi-stage fractured shale gas reservoirs with damaged fractures and stimulated reservoir volumes. *J. Petrol. Sci. Eng.* **187** (2020).
13. Youjie, X., Li, X. & Liu, Q. Pressure performance of multi-stage fractured horizontal well with stimulated reservoir volume and irregular fractures distribution in shale gas reservoirs. *J. Nat. Gas Sci. Eng.* **77** (2020).
14. Micheal, M. et al. Gas production from shale reservoirs with bifurcating fractures: A modified quadruple-domain model coupling microseismic events. *Energy* **278** (2023).
15. Zangqa, S. et al. Hydraulic fracturing potential of tight gas reservoirs: A case study from a gas field in the Bredasdorp basin, South Africa. *Gas Sci. Eng.* **128**, 13 (2024).
16. Li, X., Li, H., Qi, C. & Wu, K. A micro-macro mechanism of hydraulic fracturing with initial stress state effect of brittle rock. *Geoenergy Sci. Eng.* **241** (2024).
17. Meng, S. et al. Study on dynamic fracture growth mechanism of continental shale under compression failure. *Gas Sci. Eng.* **114** (2023).
18. Manchanda, R., Sharma, M. M. & Holzhauser, S. Time dependent fracture interference effects in pad wells. *SPE Prod. Oper.* **29**(04), 274–287 (2014).
19. Li, S. et al. Experimental study on the feasibility of supercritical CO₂-gel fracturing for stimulating shale oil reservoirs. *Eng. Fract. Mech.* **238**, 107276 (2020).
20. Zhang, B. et al. Simulation study of micro-proppant carrying capacity of supercritical CO₂ (Sc-CO₂) in secondary fractures of shale gas reservoirs. *Geoenergy Sci. Eng.* **224**, 15 (2023).
21. He Yonghong, X. et al. *Pet. Explor. Dev.*, **50**(06): 1245–1258. (2023).
22. Li Xianwen, W. & Lili, W. *Wenxiong Et Al Nat. Gas Ind.*, **42**(09): 76–83. (2022).
23. Jiang Yanfang. *Petroleum Geol. Eng.*, **36**(02): 95–100. (2022).
24. Wu Shunlin, L. et al. *Drill. Prod. Technol.*, **43**(03): 53–55. (2020).
25. Yang Zhaozhong, C. & Qian, L. *Xiaogang Et Al Petroleum Geol. Recovery Effi.*, **26**(02): 120–126. (2019).
26. Liang, X. & Gaoming, Y. *Huang Yongzhang Et Al Fault-Block Oil Gas Field*, **26**(05): 617–621. (2019).
27. Zhang, Z. et al. Optimizing fracturing techniques for enhanced hydrate dissociation in low-permeability reservoirs: Insights from numerical simulation. *Gas Sci. Eng.* **125** (2024).
28. Zhou, P. et al. Study on the shale fracture geometry influence on nonlinear gas seepage behavior. *Gas Sci. Eng.* **125** (2024).

Acknowledgements

We appreciate the support of Sinopec North China Branch Company for this work and for permission to publish this paper. This research was supported by the “Key Technologies for Drilling, Completion, and Fracturing of Tight Gas Reservoirs” project of Sinopec (P23156).

Author contributions

Guang Dong, Yanping Lu wrote the main manuscript text and Shuai Dong prepared figures. All authors reviewed the manuscript.

Declarations

Competing interests

The authors declare no competing interests.

Additional information

Supplementary Information The online version contains supplementary material available at <https://doi.org/10.1038/s41598-025-12773-2>.

Correspondence and requests for materials should be addressed to Y.L.

Reprints and permissions information is available at www.nature.com/reprints.

Publisher's note Springer Nature remains neutral with regard to jurisdictional claims in published maps and institutional affiliations.

Open Access This article is licensed under a Creative Commons Attribution-NonCommercial-NoDerivatives 4.0 International License, which permits any non-commercial use, sharing, distribution and reproduction in any medium or format, as long as you give appropriate credit to the original author(s) and the source, provide a link to the Creative Commons licence, and indicate if you modified the licensed material. You do not have permission under this licence to share adapted material derived from this article or parts of it. The images or other third party material in this article are included in the article's Creative Commons licence, unless indicated otherwise in a credit line to the material. If material is not included in the article's Creative Commons licence and your intended use is not permitted by statutory regulation or exceeds the permitted use, you will need to obtain permission directly from the copyright holder. To view a copy of this licence, visit <http://creativecommons.org/licenses/by-nc-nd/4.0/>.

© The Author(s) 2025